RESEARCH ARTICLE

Dielectric, Ferroelectric, and Optical Properties of $Sr_{0.7}Bi_{0.2}TiO_3$-Based Ceramics

Sana Fazal[1] **and Kainat Shah**[1,*]

[1] Department of Physics, Abdul Wali Khan University Mardan, 23200 KP, Pakistan

Abstract

In this work, the effect of additives (Al_2O_3, ZrO_2, and Nb_2O_5) on the dielectric and ferroelectric properties of $Sr_{0.7}Bi_{0.2}TiO_3$ (SBT) relaxor ferroelectric was investigated. Relative density of SBT was estimated to be above 95%. XRD analysis confirmed the formation of cubic perovskite structure for all the samples. P_{max} of SBT decreased by adding ZrO_2, Nb_2O_5 and Al_2O_3, while remnant polarization (P_r) and coercive field (E_c) increased. For pure SBT, the breakdown strength was 75 kV which increased to 90 kV for ZrO_2- and Al_2O_3-added SBT but decreased to 60 kV when the additive was Nb_2O_5. As Nb acts as a donor in the NBT, increasing the leakage current and reduced the breakdown strength. Overall, the recoverable energy storage density (W_{rec}) of SBT decreased with the addition of additives. It was interesting to note that the dielectric loss significantly decreased with additives. The optical band gap of SBT slightly decreased from 2.98 eV to 2.97 and 2.96 eV (for Al_2O_3 and ZrO_2 added to SBT) while it surprisingly increased to 2.99 eV when the additive was Nb_2O_5. This may be attributed to the reason optical band gap does not show the localized defect states or electrical conduction paths, thus underestimating the band gap from DRS.

Keywords: $Sr_{0.7}Bi_{0.2}TiO_3$, additives, donors, acceptors, relaxor.

1 Introduction

Currently, pulsed power systems are widely used in different fields such as medical equipment, electromagnetic pulse weapons, power electronics, hybrid electric vehicles etc. Essential element for pulsed power system is pulsed storage dielectric capacitors having outstanding reliability, high power density, long life duration and rapid charge-discharge rate. Compared to batteries, electrochemical capacitors and other energy storage devices, the relatively low energy storage density of electrostatic capacitors limits their application. Consequently, enhancing the energy storage density of pulsed storage capacitors has become a key research focus. For dielectric capacitors, a dielectric material should have high P_{max}, high W_{rec} and efficiency, low Pr, and high breakdown strength (BDS) [1–3]. Although currently ceramics and polymers are regarded as superior dielectric energy storage materials. However, due to their excellent thermal stability and mechanical properties as compared to polymers, dielectric ceramics are considered as potential candidates for dielectric

Submitted: 02 August 2025
Accepted: 30 October 2025
Published: 11 December 2025

Vol. 1, **No.** 1, 2025.
10.62762/JAEM.2025.458530

***Corresponding author:**
✉ Kainat Shah
kainat.lfmd@gmail.com

Citation
Fazal, S., & Shah, K. (2025). Dielectric, Ferroelectric, and Optical Properties of $Sr_{0.7}Bi_{0.2}TiO_3$-Based Ceramics. *Journal of Advanced Electronic Materials*, 1(1), 17–23.

capacitors.

A well-known type of dielectric materials called ferroelectrics are utilized in various fields such as: information storage, dielectric capacitors, and ferroelectric photovoltaics [4]. The relative polarization of $SrTiO_3$ (ST) is comparatively low (i.e. at 1 kHz the dielectric constant is less than 400 at room temperature) [5]. In ST, Bi^{3+} doping results in the formations of an A-site deficient perovskite $Sr_{0.7}Bi_{0.2}TiO_3$ (SBT) [6]. Bi^{3+} takes the off-center position at the A-site which enhances the polarization and hence the dielectric constant [7]. The Sr vacancies appear for valance balancing which deforms the oxygen octahedron, causing the relaxational movement of Ti^{4+}. Subsequently, the polar nano-regions (PNRs) form and SBT behave like a relaxor ferroelectric material. Compared to other ferroelectric materials (e.g., $BaTiO_3$), or antiferroelectric materials (e.g., $AgNbO_3$), SBT has better characteristics like increased energy density and efficiency, and decreased remanent polarization [8]. For energy storage, SBT experiences many advantages like; in a broad range of temperatures, it shows excellent ferroelectric relaxor behavior and diffused dielectric maximum, resulting from the Bi^{3+} ion off centering [9–12]. In contrast, low saturation polarization is one of the drawbacks of SBT-based ceramics. Polarization and BDS are the two main considerable parameters for ferroelectric energy storage ceramics. As the energy storage density of SBT-based ceramics is limited by the relatively low BDS, so for maximum energy storage performance, the importance of high BDS must be emphasized. To enhance the performance of SBT, many studies have been conducted and reported in the literature. Introducing Ca^{2+} in SBT lattice (SBT-XC, where x = 0 to 0.15) decreased the conductivity and leakage current while increasing the oxygen vacancies and enhancing BDS, dielectric constant and relaxor properties of the SBT. For x = 0.1, the sample exhibited a high BDS of 480.2 kV/cm, W_{rec} of 2.1 J/cm^3 with an efficiency of 97.6%, and maximum P_D (power density) of 50.1 MW/cm^3, making this composition a potential candidate for dielectric capacitors [13]. Substituting Ta_2O_5 at the B-site of SBT ($Sr_{0.7}Bi_{0.2}Ti_{(1-1.25x)}Ta_xO_3$ or SBT-T) introduces B-site ion disorder which in turn boosts activation energy, impedance and relaxor behavior of SBT-T ceramics, hence improving their BDS. By increasing Ta content in the composition, the critical electric fields were increased by 54% (from 240 to 370 kV/cm), and recorded W_{rec} of 2.33 J/cm^3 and efficiency of 91.76% at 290 kV/cm. Moreover, at x = 0.04, SBT-T ceramics exhibited maximum P_D = 153.39 MW/cm^3 and enhanced charge-discharge rate of 81.69 ns [5]. Apart from doping strategy, some are based on synthesis of binary and ternary solid solutions [12, 14–19]. However, there are very few studies on the additives based SBT; therefore, in the present study, isovalent (ZrO_2), acceptor (Al_2O_3) and donor (Nb_2O_5) were added to the SBT to enhance the ferroelectric properties of SBT.

2 Experimental procedures

$Sr_{0.7}Bi_{0.2}TiO_3$ (SBT) ceramics and SBT with 1 mol% additives (ZrO_2, Nb_2O_5, and Al_2O_3) were synthesized via the conventional solid-state sintering route. Bi_2O_3 (99.9%, Sigma Aldrich), Nb_2O_5 (99.9%, Sigma Aldrich), Al_2O_3 (99.9%, Sigma Aldrich), TiO_2 (99%, Sigma Aldrich) powders, and ZrO_2 (99%, UNI-CHEM) were used as starting precursors. The precursors were weighed according to the specific stoichiometric ratios and mixed thoroughly using an agate mortar and pestle in an anhydrous acetone medium for 3 hours to ensure homogeneity. The homogenized mixture was calcined at 950 °C for 3 h in a muffle furnace. Post-calcination, the powders were ground again for 1 h in an agate mortar and pestle to break up agglomerates and reduce particle size, thereby increasing the surface area. Cylindrical pellets were formed using a hydraulic press under a pressure of 25 bar. These green pellets were sintered at 1250 °C for 3 h in a muffle furnace to achieve densification.

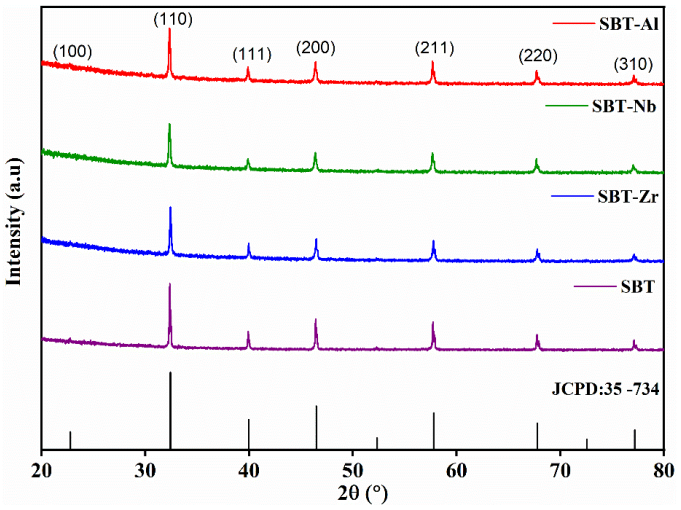

Figure 1. XRD patterns of SBT-based samples.

Density of the samples was measured using Archimedes principle. X-ray diffraction (XRD) data were collected using a Proto X-ray Diffractometer with Cu-Kα radiation ($\lambda = 1.5406$ Å) over a 2θ range

Table 1. Overall densities calculation of SBT, SBT-Zr, SBT-Nb and SBT-Al.

Sample	Observable Density ($g\,cm^{-3}$)	Theoretical Density ($g\,cm^{-3}$)	Relative density (%)
SBT	–	–	93.3 [10]
SBT	5.17	5.44	95
SBT-Zr	5.4	5.50	98
SBT-Nb	5.35	5.49	97.4
SBT-Al	5.33	5.48	97.2

of 20° to 80°, with a step size of 0.02°, to study the crystal structure and phase formation. For dielectric measurement, pellets were coated with silver on both sides. The relative permittivity and dielectric loss were measured in the frequency range of 10 Hz to 1 MHz using a Microtest-6630 LCR meter. Ferroelectric properties were investigated by recording P–E hysteresis loops at room temperature at a frequency of 10 Hz using a PolyK ferroelectric analyzer coupled with a Trek high-voltage amplifier. The optical properties of the samples were investigated by using PerkinElmer DRS (365).

3 Results and Discussion

Figure 1 shows the XRD patterns of SBT, SBT-Zr, SBT-Nb, and SBT-Al ceramics. The patterns match JCPDS card no. 35-734, confirming a cubic perovskite structure for all samples. The appearance of a single phase and the absence of any secondary phases in all compositions suggest that the additives are either fully soluble in the SBT matrix or present in amounts below the detection limit of the in-house XRD facility.

The observed density of the samples was determined using Archimedes' method. After sintering at 1250 °C for 3 h, pure SBT exhibited a relative density of approximately 95%, as shown in Table 1. Furthermore, the addition of a small amount (1 mol%) of ZrO_2, Nb_2O_5, and Al_2O_3 at the same sintering temperature led to an improvement in the densification process, resulting in increased relative densities. This enhancement in density is beneficial for reducing defects and porosity, which can significantly influence the dielectric and ferroelectric properties of the ceramics.

At room temperature, the relative permittivity (ε_r) and dielectric loss ($\tan\delta$) as a function of frequency for pure SBT ceramics, in the range of 1 kHz to 1 MHz, are shown in Figure 2(a). At low frequency, the maximum dielectric constant is approximately 770, which decreases with increasing frequency. This reduction in ε_r is attributed to the diminishing contribution of space charge polarization mechanisms at higher frequencies. Similarly, the dielectric loss ($\tan\delta$) is initially high ($\sim$0.062) but gradually decreases with frequency, reaching a lower value of $\sim$0.036 at 1 MHz. The frequency-dependent dielectric behavior of SBT-based composites is presented in Figure 2(b, c and d). The results demonstrate that both ε_r and $\tan\delta$ decrease as the frequency increases from 1 kHz to 1 MHz, consistent with typical dielectric relaxation behavior due to the reduced contribution of slower polarization mechanisms at higher frequencies. At low frequencies, the maximum values of ε_r are approximately 579 for SBT-Zr, 587 for SBT-Al, and 445 for SBT-Nb. At high frequencies, the ε_r values stabilize around 537 for SBT-Zr, 533 for SBT-Al, and 426 for SBT-Nb. Regarding dielectric loss, the maximum values observed at low frequencies are $\sim$0.037 for SBT-Zr, $\sim$0.033 for SBT-Al, and $\sim$0.066 for SBT-Nb. These values decrease at higher frequencies, reaching minimum stable values of approximately 0.020 for both SBT-Zr and SBT-Al, and 0.015 for SBT-Nb. The observed reduction in dielectric loss across all SBT-based composites indicates that the addition of small amounts of ZrO_2, Nb_2O_5, and Al_2O_3 effectively enhances the dielectric resistivity of pure SBT by reducing charge carrier mobility and associated leakage currents.

Different ferroelectric parameters, including maximum polarization (P_{max}) or saturation polarization (P_{sat}), remnant polarization (P_r), coercive field (E_c), and energy storage properties of the materials, were calculated from the P–E hysteresis loops, as presented in Table 2. The slim P–E loop of pure SBT (Figure 3(a)) indicates its relaxor ferroelectric behavior, with a maximum breakdown strength (BDS) of 75 $kV\,cm^{-1}$. At low electric fields, the energy storage capability and polarization are relatively small, resulting in a narrow loop. As the electric field gradually increases, the P–E loop expands, indicating enhanced polarization. The total energy storage density (W_t) of pure SBT was found to

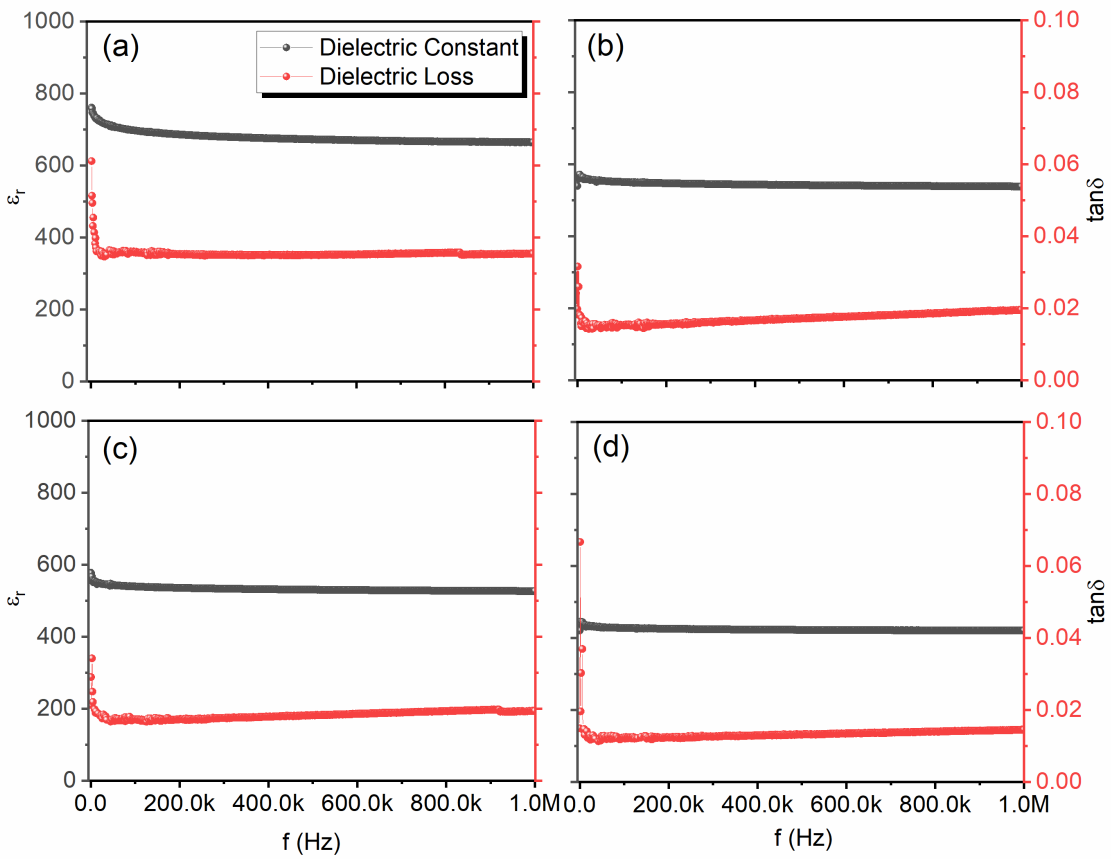

Figure 2. Variation of ε_r and $\tan\delta$ as a function of frequency for (a) SBT, (b) SBT-Zr, (c) SBT-Al and (d) SBT-Nb.

Table 2. Total energy storage density (W_t) and W_{rec} of SBT, SBT-Zr, SBT-Al and SBT-Nb.

Composition	Maximum Breakdown Voltage ($kV\,cm^{-1}$)	Energy Storage Density W_t ($J\,cm^{-3}$)	Recoverable Energy Storage Density W_{rec} ($J\,cm^{-3}$)
SBT	75	0.307	0.239
SBT-Zr	90	0.407	0.152
SBT-Al	90	0.291	0.167
SBT-Nb	60	0.135	0.079

increase up to $0.307\,J\,cm^{-3}$.

To further improve the BDS of SBT, 1 mol% ZrO_2, Al_2O_3, and Nb_2O_5 were incorporated, which also contributed to reducing grain size. A higher BDS is beneficial for achieving greater energy storage density. The results show that the breakdown strength effectively increased for SBT-Zr and SBT-Al, reaching $90\,kV\,cm^{-1}$, but decreased for SBT-Nb to $60\,kV\,cm^{-1}$ (see Figure 3(d)). The reduction in BDS for SBT-Nb is attributed to the Nb donor, which introduces electronic charge carriers, suppressing oxygen-vacancy related AC loss but may enhance DC assisted conduction through grain boundary. Hence, BDS decreased due to increased conduction path at high field stress. The addition of ZrO_2, Al_2O_3, and Nb_2O_5 resulted in a reduction in P_{max}, while P_r and E_c increased relative to pure SBT. In terms of energy storage performance, SBT-Zr exhibited the highest total energy storage density of $0.407\,J\,cm^{-3}$, whereas SBT-Al and SBT-Nb showed decreased values of $0.291\,J\,cm^{-3}$ and $0.135\,J\,cm^{-3}$, respectively. Additionally, the recoverable energy density (W_{rec}) also decreased for the composites, as summarized in Table 2.

At the electronic level, the band gap (E_g) is one of the intrinsic characteristics that influences the breakdown strength (BDS) of a material [20]. In this work, the band gap of SBT ceramics and their composites was calculated using Diffuse Reflectance Spectroscopy (DRS). For the pure SBT sample, the E_g calculated from the $(\alpha h\nu)^2$ versus $h\nu$ plot was found to be 2.98 eV (as shown in Figure 4), which is higher than the value reported in the literature (see Table 3). A larger E_g

Table 3. P_{max}, P_r, and E_c values at 60 kV, and optical band gap values of SBT-based samples.

Component	Maximum Polarization P_{max} ($\mu C\,cm^{-2}$)	Remnant Polarization P_r ($\mu C\,cm^{-2}$)	Coercive field E_c ($kV\,cm^{-1}$)	Band gap (eV)
SBT	6.34	0.51	4.05	2.98
SBT-Zr	4.77	1.13	9.99	2.96
SBT-Nb	3.82	0.72	9.62	2.99
SBT-Al	3.71	0.58	5.97	2.97

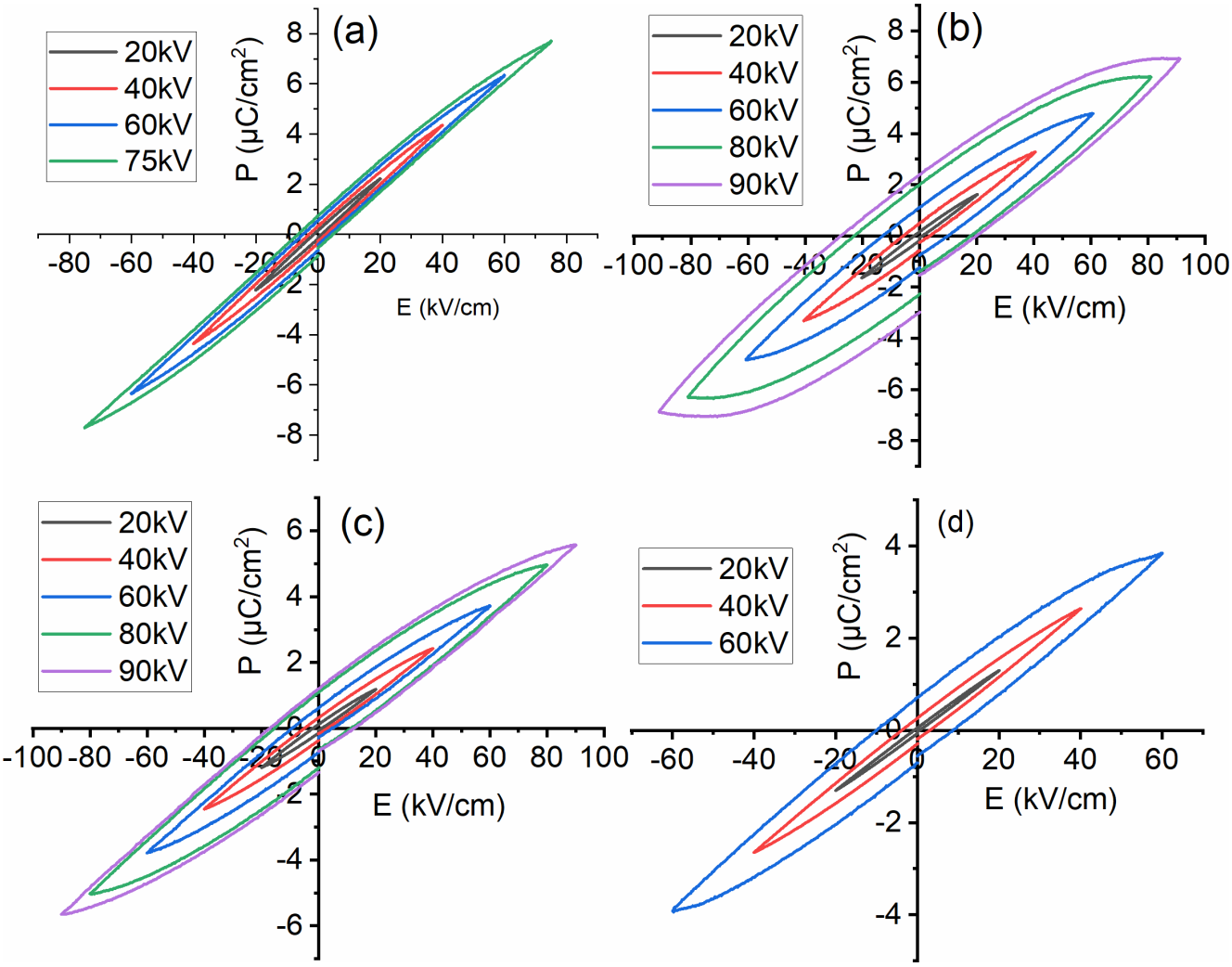

Figure 3. P-E loop of a) SBT, b) SBT-Zr, c) SBT-Al, and d) SBT-Nb ceramics.

typically leads to higher BDS, reduced leakage current, and increased resistance, as it makes it more difficult for electrons to transition from the valence band (VB) to the conduction band (CB) [21]. However, the E_g values decreased in the case of SBT-based composites (SBT-Zr, SBT-Al) compared to pure SBT. The observed E_g values for SBT-Zr, SBT-Al, and SBT-Nb composites were 2.96 eV, 2.97 eV, and 2.99 eV, respectively. The increase in the band gap of SBT-Nb based system may be due to the reason optical band gap does not show the localized defect states or electrical conduction paths, thus underestimating the band gap from DRS.

4 Conclusion

Lead-free relaxor ferroelectric SBT ceramics and their composites (SBT-Zr, SBT-Al, and SBT-Nb) with a cubic perovskite structure were successfully fabricated via the conventional solid-state reaction route. XRD analysis confirmed the absence of secondary phases in the SBT-based composites, indicating that the additives sintered at 1250 °C for 3 h were successfully incorporated into the SBT crystal structure. The relative density of pure SBT improved from 95% upon additive incorporation, reaching a maximum of

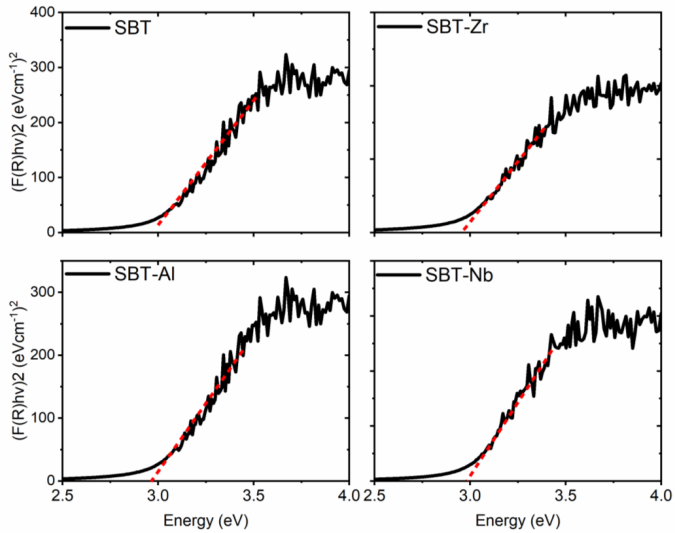

Figure 4. Tauc plots for SBT, SBT-Zr, SBT-Al, and SBT-Nb samples.

98% in SBT-Zr and 97% in both SBT-Nb and SBT-Al. A noticeable enhancement in breakdown strength (BDS) was observed upon the addition of small amounts of ZrO_2 and Al_2O_3, increasing the breakdown voltage from 75 kV to 90 kV. However, the addition of Nb_2O_5 reduced the breakdown voltage to 60 kV. This reduction may be attributed to the donor Nb^{5+}, which generate defects and free electrons, thereby degrading the insulating properties and increasing leakage current. The pure SBT sample exhibited a wide band gap of 2.98 eV, contributing to its superior insulating behavior, thermal stability, low leakage current, and high energy storage efficiency. Upon the addition of the dopants (Al_2O_3 and ZrO_2), the band gap decreased to approximately 2.97 eV and 2.96 eV while in the case of Nb_2O_5, it again increased to 2.99 eV. The incorporation of ZrO_2, Nb_2O_5, and Al_2O_3 in pure SBT reduced the maximum polarization from $6.34\,\mu C\,cm^{-2}$ to $4.77\,\mu C\,cm^{-2}$, $3.83\,\mu C\,cm^{-2}$, and $3.71\,\mu C\,cm^{-2}$, respectively, while increasing the remnant polarization from $0.51\,\mu C\,cm^{-2}$ to $1.13\,\mu C\,cm^{-2}$, $0.72\,\mu C\,cm^{-2}$, and $0.58\,\mu C\,cm^{-2}$. As a result, the recoverable energy density (W_{rec}) of SBT decreased from $0.239\,J\,cm^{-3}$ to $0.167\,J\,cm^{-3}$, $0.152\,J\,cm^{-3}$, and $0.079\,J\,cm^{-3}$ for SBT-Zr, SBT-Al, and SBT-Nb, respectively. Furthermore, although the additives slightly decreased the dielectric constant of SBT, they also significantly reduced the dielectric loss from 0.036 to ~0.02 in the cases of SBT-Zr and SBT-Al, and to ~0.015 in the case of SBT-Nb at high frequencies.

Data Availability Statement

Data will be made available on request.

Funding

This work was supported without any funding.

Conflicts of Interest

The authors declare no conflicts of interest.

Ethical Approval and Consent to Participate

Not applicable.

References

[1] Bin, C., Hou, X., Liao, L., Liu, Y., Yang, H., Liu, Y., & Wang, J. (2023). Improved energy storage performance in rare-earth modified lead-free BNT-based relaxor ferroelectric ceramics. *Applied Physics Letters, 123*(1). [CrossRef]

[2] Han, D., Duan, L., Wang, C., Yuan, L., Muhammad, R., Ma, P., ... & Meng, F. (2024). Effective regulation of breakdown strength through the synergistic effect of defect chemistry and energy band engineering in Ba 0.85 Ca 0.15 Zr 0.1 Ti 0.9 O 3-based lead-free ceramics. *Inorganic Chemistry Frontiers, 11*(7), 2058-2070. [CrossRef]

[3] Li, S., Guo, Q., Su, C., Liu, Y., Yao, Z., Cao, M., ... & Hao, H. (2025). Enhanced energy storage performances of (1-x) Ba0. 85Ca0. 15Zr0. 1Ti0. 9O3-xBiGaO3 lead-free ceramics and MLCC device via multiscale synergistic optimization strategy. *Chemical Engineering Journal*, 170141. [CrossRef]

[4] Bian, S., Yue, Z., Shi, Y., Zhang, J., & Feng, W. (2021). Ultrahigh energy storage density and charge-discharge performance in novel sodium bismuth titanate-based ceramics. *Journal of the American Ceramic Society, 104*(2), 936-947. [CrossRef]

[5] Li, Y., Liu, J., Zeng, M., Li, H., & Chen, J. (2023). Relaxor properties and breakdown strength of Ta doped Sr0.7Bi0.2TiO3-based lead-free ceramics for energy storage applications. *Journal of Materials Science, 58*(44), 16195-16207. [CrossRef]

[6] Zhu, X., Shi, P., Kang, R., Li, S., Wang, Z., Qiao, W., ... & Lou, X. (2021). Enhanced energy storage density of Sr0. 7BixTiO3 lead-free relaxor ceramics via A-site defect and grain size tuning. *Chemical Engineering Journal, 420*, 129808. [CrossRef]

[7] Singh, A., Moriyoshi, C., Kuroiwa, Y., & Pandey, D. (2013). Visualization of Bi3+ off-centering in the average cubic structure of (Ba0. 70Bi0. 30)(Ti0. 70Fe0. 30) O3 at the electron density level. *Applied Physics Letters, 103*(12). [CrossRef]

[8] Liu, Z. G., Li, M. D., Tang, Z. H., & Tang, X. G. (2021). Enhanced energy storage density and efficiency in lead-free Bi (Mg1/2Hf1/2) O3-modified BaTiO3 ceramics. *Chemical Engineering Journal, 418*, 129379. [CrossRef]

[9] Li, J., Li, F., Xu, Z., & Zhang, S. (2018). Multilayer lead-free ceramic capacitors with ultrahigh energy density and efficiency. *Advanced Materials, 30*(32), 1802155. [CrossRef]

[10] Sakurai, M., Kanehara, K., Takeda, H., Tsurumi, T., & Hoshina, T. (2016). Wideband dielectric spectroscopy of (Sr0. 7Bi0. 2) TiO3 ceramics and its microscopic mechanism of polarization. *Journal of the Ceramic Society of Japan, 124*(6), 664-667. [CrossRef]

[11] Zhang, G. F., Cao, M., Hao, H., & Liu, H. (2013). Energy storage characteristics in Sr (1-1.5 x) BixTiO3 ceramics. *Ferroelectrics, 447*(1), 86-94. [CrossRef]

[12] Su, Q., Zhu, J., Ma, Z., Meng, X., Zhao, Y., Li, Y., & Hao, X. (2022). Enhanced energy-storage properties and charge-discharge performances in Sm3+ modified (Na0. 5Bi0. 5) TiO3-SrTiO3 lead-free relaxor ferroelectric ceramics. *Materials Research Bulletin, 148*, 111675. [CrossRef]

[13] Zhao, P., Tang, B., Si, F., Yang, C., Li, H., & Zhang, S. (2020). Novel Ca doped Sr0. 7Bi0. 2TiO3 lead-free relaxor ferroelectrics with high energy density and efficiency. *Journal of the European Ceramic Society, 40*(5), 1938-1946. [CrossRef]

[14] Zhang, G. F., Liu, H., Yao, Z., Cao, M., & Hao, H. (2015). Effects of Ca doping on the energy storage properties of (Sr, Ca) TiO3 paraelectric ceramics. *Journal of Materials Science: Materials in Electronics, 26*(5), 2726-2732. [CrossRef]

[15] Chen, J., Zhao, P., Si, F., Li, Y., Zhang, S., Fang, Z., & Tang, B. (2024). Optimizing electrical performance of low hysteresis Sr0. 7Bi0. 2TiO3 energy storage ceramic. *Ceramics International, 50*(8), 13208-13218. [CrossRef]

[16] Kong, X., Yang, L., Cheng, Z., & Zhang, S. (2021). Enhanced energy-storage properties and good temperature stability in 0.92(Sr0.7Bi0.2TiO3–0.08Bi(Mg0.5Hf0.5)O3 relaxor ferroelectric ceramic. *Advanced Energy and Sustainability Research, 2*(6), 2100015. [CrossRef]

[17] Yao, K., Zhou, C., Wang, J., Li, Q., Yuan, C., Xu, J., Chen, G., & Rao, G. (2021). A new strategy to realize high energy storage properties and ultrafast discharge speed in Sr0.7Bi0.2TiO3-based relaxor ferroelectric ceramic. *Journal of Alloys and Compounds, 883*, 160855. [CrossRef]

[18] Li, Y., Liu, J., Zeng, M., Li, H., & Yuan, Y. (2024). Enhanced relaxor behavior and excellent anti-fatigue performance in lanthanum-modified Sr0.7Bi0.2TiO3 ceramics. *Materials Today Communications, 41*, 110872. [CrossRef]

[19] Zhao, P., Fang, Z., Zhang, X., Chen, J., Shen, Y., Zhang, X., ... & Tang, B. (2021). Aliovalent doping engineering for A-and B-sites with multiple regulatory mechanisms: a strategy to improve energy storage properties of Sr0. 7Bi0. 2TiO3-based lead-free relaxor ferroelectric ceramics. *ACS applied materials & interfaces, 13*(21), 24833-24855. [CrossRef]

[20] Kong, X., Yang, L., Cheng, Z., & Zhang, S. (2020). Bi-modified SrTiO3-based ceramics for high-temperature energy storage applications. *Journal of the American Ceramic Society, 103*(3), 1722-1731. [CrossRef]

[21] Sun, Y., Boggs, S., & Ramprasad, R. (2012). The intrinsic electrical breakdown strength of insulators from first principles. *Applied Physics Letters, 101*(13). [CrossRef]

Sana Fazal has completed her MPhil under the supervision of Prof. Raz Muhammad at the Department of Physics at Abdul Wali Khan University Mardan, Pakistan. Her research focuses on dielectric and ferroelectric materials for energy storage applications, with a special interest in lead-free perovskite ceramics. She has been actively involved in the synthesis and characterization of advanced functional materials, including relaxor ferroelectrics and optical ceramics. (Email: sanafazalphy@gmail.com)

Kainat Shah is an MPhil scholar, working under the supervision of Prof. Raz Muhammad at the Department of Physics at Abdul Wali Khan University Mardan, Pakistan. Her research areas include dielectric materials, multiferroics, and energy storage systems. She is currently supervising multiple undergraduate research projects in the field of ferroelectric and composite based materials. She is currently engaged in research on hybrid (organic-inorganic) lead-free energy storage materials. (Email: lfmd@awkum.edu.pk)